Mapping Protease Susceptibility Sites on the *Escherichia coli* Transcription Factor σ^{70}†

Scott A. McMahan‡ and Richard R. Burgess*

McArdle Laboratory for Cancer Research, University of Wisconsin−Madison, Madison, Wisconsin 53706

Received April 9, 1999; Revised Manuscript Received July 14, 1999

ABSTRACT: N-terminally and C-terminally histidine-tagged versions of *Escherichia coli* RNA polymerase initiation factor σ^{70} were subjected to limited proteolysis and electrophoretic separation. The protein fragments were transferred to nitrocellulose, and biotinylated nitrilotriacetic acid was used to detect the His-tagged ladder that resulted. Using size markers of known lengths derived from chemical cleavage of the same His-tagged σ^{70}, we were able to map the sites of proteolysis for σ^{70} free in solution, bound to core RNA polymerase, and in the Mg^{2+}-dependent open complex with λP_R promoter DNA. Numerous sites of changed susceptibility were mapped. Most of these sites mapped near residues 100 and 500. In addition, the highly acidic region around residue 190 became susceptible to cleavage in the open promoter complex. These results suggest that σ^{70} undergoes significant conformational changes upon binding to core RNA polymerase and upon open promoter complex formation.

Transcription initiation in *Escherichia coli* is under the control of a family of proteins known as σ factors (*1*). These proteins work in a cyclic fashion. Originally, σ^{70} was recognized to be involved in at least three steps in this cycle (*2*). Since then, additional steps have been added, so there are now at least seven. Free σ^{70} binds to core RNA polymerase, which has the subunit structure $\alpha_2\beta\beta'$ (*3, 4*). This holoenzyme binds to promoter DNA and isomerizes through at least three kinetically distinct forms, two of which are distinguished by the presence or absence of Mg^{2+} (*5, 6*). After isomerization, initiating NTPs bind, transcription initiation begins, and the σ^{70} is released.

Little is currently known about the conformational changes that σ^{70} goes through as it passes through these steps. X-ray crystallography has been used to determine the three-dimensional structure of a σ^{70} fragment consisting of residues 114−448 (*7*). While this has greatly advanced our understanding of the structure of part of σ^{70}, there is still a great deal left to learn. The crystal structure is a snapshot of one conformation of approximately half of the full-length protein.

Likewise, it has yet to be determined which sites on σ^{70} are involved in core binding. While a 30-residue stretch that overlaps region 2.1 has been shown to be necessary and sufficient for core binding (*8*), it seems unlikely that this is the only region of σ^{70} involved in core binding. A deletion mutant of the alternative σ factor, σ^{32}, has been shown to have reduced affinity for core (*9*); however, this mutation could be indirectly affecting core binding (*10, 11*).

To better understand what is happening to σ^{70} in some of its various kinetic states, we have performed limited proteolysis on N-terminally and C-terminally His-tagged σ^{70} free in solution, bound to core in the holoenzyme, and bound to promoter DNA in the Mg^{2+}-dependent open complex. We then examined the sites of protease susceptibility by specifically detecting the ladder of His-tagged fragments that resulted. Based on these results, we are able to support some previously proposed models concerning the structure of σ^{70} as well as add some new ideas.

EXPERIMENTAL PROCEDURES

Commercial Chemicals and Enzymes. Pyrococcus furiosus DNA polymerase for PCR was purchased from Stratagene. NTCB[1] and the proteases bromelain, elastase, and papain were purchased from Sigma. Cucumisin and thermolysin were from Calbiochem. Insulin was from Boehringer-Mannheim. The proteases were dissolved in protease buffer (10 mM Hepes, pH 7.3, and 0.1 mM DTT) to the stock concentrations given in Table 1 without further purification and stored at −20 °C until use.

Plasmids. (A) pCJ-3. The construction of pCJ-3, which codes for a 10-histidine tag plus 12 additional residues upstream of the *E. coli* σ^{70} gene, *rpoD*, under control of a T7 polymerase promoter in plasmid pET19b (Novagen), has been described previously (*14*).

(B) pLHN12CH. Construction of pLHN12CH, which codes for *rpoD* followed by 6 histidine residues, began with pLHN12 (*14*), coding for *rpoD* in pET11T (*15*). This was digested with *Xba*I and *Eco*RI, and the fragment was inserted into the same sites as part of the multiple cloning sites in pSP65 (Promega), producing pLHN11. pMRG8 (*16*) was

† This work was supported by NIH Grants GM 28575 and CA 09230.

* To whom correspondence should be addressed. Email: burgess@oncology.wisc.edu.

‡ Current address: Institute for Enzyme Research, University of Wisconsin, Madison, WI 53715.

[1] Abbreviations: αCTD, C-terminal domain of the α subunit of core RNA polymerase; BNTA, biotinylated nitrilotriacetic acid; Gu·HCl, guanidinium chloride; His-tag, 6 histidine tag on N- or C-terminus of a protein; NTCB, 2-nitro-5-thiocyanobenzoic acid; TCA, trichloroacetic acid; TE, 10 mM Tris·HCl, pH 7.9, 0.1 mM EDTA; Tris·HCl, tris-(hydroxymethyl)aminomethane hydrochloride.

10.1021/bi990824x CCC: $18.00
Published on Web 08/31/1999

Table 1: Proteases Used in This Study

protease[a]	specificity[b]	stock concn	rel act. (%) with DNA added
bromelain	A′X, G′X	320 mU/mL	97
cucumisin	D′X, E′X, N′X, Q′X	750 U/mL	106
elastase	I′X > V′X > A′X	22 U/mL	94
ficin	A′X, G′X, L′X	340 mU/mL	ND[c]
papain	very wide	84 mU/mL	88
subtilisin	broad	50 mU/mL	ND
S. aureus V8	E′X > D′X	32 U/mL	ND
thermolysin	X′I, X′L, X′V, X′A, X′M, X′F	50 pU/mL	103
trypsin	R′X > K′X	14 U/mL	ND

[a] Information source: cucumisin, (*10*); all others, (*11*). [b] X indicates any amino acid. A slanted prime indicates cleavage with respect to the preferred cleavage site. [c] Activity not determined.

used as a template for generation of a PCR-generated fragment using a 54-base primer starting 30 base pairs upstream of *rpoD* and a second primer which added the codons for an additional 6 histidines, a termination codon, and an ***Eco***RI site at the C-terminus of *rpoD*. This fragment and pLHN11 were digested with *Xho*I and *Eco*RI and ligated together to form pLHN11CH. The PCR-generated region was sequenced, and no mutations were found. The *Xba*I to *Eco*RI fragment of pLHN11CH was then cloned into pET16b (Novagen) under T7 RNA polymerase control.

(C) pBR81. pBR81 is a plasmid containing a synthetic λP_R. Its construction has been detailed elsewhere (*17*) and was the kind gift of the Thomas Record lab.

Protein Purification. Core RNA polymerase was purified using immunoaffinity chromatography (*18*) which resulted in a mixture of core and various holoenzymes. These were pooled and run over a Bio-Rex 70 column (Bio-Rad) to separate σ^{70} and most minor σ factors from the core enzyme (*19*). The core fraction was collected and rerun over the Bio-Rex 70 column. The purified core was dialyzed against polymerase storage buffer (40 mM Tris-HCl, pH 7.9, 0.1 mM EDTA, 0.1 mM DTT, 50% glycerol, 0.1 M NaCl; *19*) and stored at −80 °C until use. Purification of both C-His-tagged and N-His-tagged *E. coli* σ^{70} from inclusion bodies by solubilization in Gu·HCl and refolding by gradual 64-fold dilution was performed as described (*14*).

λP_R DNA Purification. Primers corresponding to base pairs −209 to −187 and +125 to +147 relative to the transcription start site of the λP_R promoter in pBR81 were used in 100 μL PCR reactions to generate a 356 bp fragment containing the λP_R promoter. The reactions were combined 40 at a time, phenol extracted, ethanol precipitated, and dissolved in 50 μL of TE. The promoter fragment was then purified by running over a 40 × 2.5 cm Sephacryl 500-HR (Pharmacia) sizing column using TE as the mobile phase. The peak containing the purified fragment was concentrated in a Centricon 30 (Amicon) until spectrophotometric assays indicated the concentration was greater then 22 pmol/μL. The sample was then diluted with TE to 22 pmol/μL and stored at 4 °C.

Detection of His-tagged σ^{70} with Biotinylated Nitrilotriacetic Acid. BNTA, a biotin derivative which contains a Ni^{2+} chelation site for binding His-tagged proteins, was synthesized and used in a manner analogous to a biotinylated antibody in immunoblotting as described previously (*20*). The biotin was detected using a NeutrAvidin−HRP conjugate (Molecular Probes).

Formation of Free His-tagged σ^{70}, His-tagged σ^{70} Holo RNA Polymerase, and His-tagged σ^{70} Open Promoter Complexes. Five microliters of either 10 mg/mL insulin (free σ^{70}) or 7.8 mg/mL insulin (holoenzyme and open complex) in water was added to 21.8 μL of H_2O. To this was added 5 μL of 10× reaction buffer (0.1 M $MgCl_2$, 0.5 M NaCl, 0.4 M Hepes, pH 7.3, 1.0 mM DTT, 1.0 mM EDTA, and 0.1% Triton X-100). Then 11.4 μL of 1 mg/mL core RNA polymerase (holoenzyme and open complex) or polymerase storage buffer (free σ^{70}) was added. Next 3.6 μL of 0.36 mg/mL His-tagged σ^{70} was added to each reaction; 3.2 μL of TE was added to the samples lacking DNA, while the open complex samples received an equivalent volume of 5.2 mg/mL (22 pmol/μL) λP_R fragment. Samples were then heated for 5 min at 37 °C. The molar ratios of key components in these reactions (when present) were 1 σ^{70} to 1.7 core to 3.9 promoter. σ^{70} was present at a final concentration of 26 μg/mL or 0.37 μM. The final conditions were 40 mM Hepes, pH 7.3, 10 mM $MgCl_2$, 80 mM NaCl, 0.13 mM DTT, 0.14 mM EDTA, 0.01% Triton X-100, 15% glycerol, and 3.6 mM Tris. The final volume was 50 μL.

Assay for His-tagged σ^{70} Holoenzyme Formation. Samples of His-tagged σ^{70} holoenzyme were formed as described above. To these samples was added 2 μL of protease buffer. The samples were applied to a 4−15% native (nondenaturing) gel for the PhastSystem (Pharmacia) and electrophoresed according to the manufacturer's protocol. The gels were either stained with Coomassie Brilliant Blue or transferred to nitrocellulose, probed with BNTA, and then stripped and probed immunologically with an anti-β' monoclonal antibody (NT73, *18*) using standard immunological techniques (*21*).

Chemical Digests of His-tagged σ^{70}. Inclusion bodies of His-tagged σ^{70} were prepared and dissolved in 8 M urea to a concentration of 5 mg/mL. These samples were then used as follows:

(A) NTCB. Fifteen microliters of His-tagged σ^{70} was added to 80 μL of 10 M urea, 4 μL of 2 M Tris·HCl, pH 9.0, and 1 μL of 1 M DTT. This solution was heated at 37 °C for 1 h. At that point, 160 μL of 10 M urea, 20 μL of 2 M Tris·HCl, pH 9.0, 20 μL of H_2O, and 1.1 mg of NTCB were added, and the digestion was allowed to proceed for 20 h at room temperature. The samples were then stored frozen at −20 °C until use.

(B) CNBr. A 0.25 mg sample of His-tagged σ^{70} was incubated 6.5 h in a 1.0 mL solution of 70% HCO_2H with 0.34 mg of CNBr. The samples were dried in a Speedvac and redissolved in 750 μL of 2 M Tris base. To this was added 500 μL of 3× Tris−Tricine sample buffer. The samples were heated for 4 min at 68 °C and stored at −20 °C.

(C) HCO_2H. Formic acid digests of His-tagged σ^{70} were performed under similar conditions to the CNBr digest, except no CNBr was added and the digestion time was lengthened to 24 h.

Proteolytic Digests. Samples of free His-tagged σ^{70}, His-tagged σ^{70} holo, and His-tagged σ^{70} holoenzyme open promoter complex were prepared as detailed above. Immediately after the 5 min incubation at 37 °C, 2 μL of protease at the stock concentration given in Table 1 was added. The samples were returned to 37 °C for an additional

1.0 min, and 25 μL of 3× Tris−Tricine sample buffer preheated to 68 °C was added and the solution was incubated for 4 min at 68 °C. The concentration of protease was determined by comparing several different concentrations and choosing a level where greater than 75% of the His-tag signal migrated as full-length σ^{70} to ensure single-hit proteolysis. The protease concentrations in Table 1 were chosen from a series of trial concentrations so that greater than 95% of the signal was seen as full-length σ^{70} when the time of exposure to X-ray film was short enough that the signal did not overexpose the film.

Assay for Effect of DNA on Protease Activity. To verify that the addition of DNA would not have an effect on the activity of the proteases used, we determined the activity of each enzyme in the presence or absence of DNA. A fluorescently labeled casein assay (PanVera) was used in the same buffer conditions as the limited proteolysis of σ^{70}. No insulin was present in these samples. Samples had either TE or 5.2 mg/mL calf thymus DNA (Sigma) added. After 1 h digest at 37 °C, samples were TCA-precipitated, and the supernatant was neutralized using the buffer provided by the manufacturer and their absorbance read at 492 nm, according to the manufacturer's protocol. To correct for the effect of the DNA on the TCA precipitation, samples of cucumisin digests lacking any DNA had TE or DNA added after digestion but before TCA precipitation, and the relative absorbances were determined. For all protease assays, signals were the average of two independent trials.

Analysis of Proteolytic Samples. Digest samples were loaded on a 25 cm long Tris−Tricine 6−12% gradient polyacrylamide gel prepared using the buffer modifications of (*22*). Samples were run until the dye front reached the bottom of the gel for C-His-tagged samples, or until a prestained marker corresponding to myoglobin was just run off the gel for N-His-tagged samples. Gels were then transferred using a Bio-Rad Trans-Blot SD semi-dry electrophoretic transfer cell to a 0.05 μm nitrocellulose membrane (Scheicher & Schuell) using the maximum settings recommended by the manufacturer. The blot was then probed with biotinylated nitrilotriacetic acid to detect His-tagged protein fragments and visualized via chemiluminescence (Boehringer-Mannheim).

Determination of Cleavage Sites. For each gel run, the logarithms of the number of residues for each marker band were plotted as a function of the distance migrated relative to the full-length σ^{70} protein. A linear regression analysis was performed, and the resulting equation was used to predict the logarithm of the number of residues in the bands generated by the proteases based on the distance migrated relative to full-length σ^{70}. In general, the position of the cleavage, given as amino acid position on σ^{70}, was accurate to within ±10 residues. It was critical to use MW markers generated by specific cleavage of His-tagged σ^{70} since the mobilities of σ^{70} and its fragments are very abnormal on SDS gels (*14*, *23*).

RESULTS

His-tagged σ^{70} Holoenzyme Formation. To determine the relative amount of His-tagged σ^{70} in the form of holoenzyme versus that still free in solution in samples where core RNA polymerase had been added, aliquots from the free His-tagged σ^{70} and the His-tagged σ^{70} holoenzyme were run on a nondenaturing polyacrylamide gel. Because of the highly acidic nature of σ^{70} (*24*), it migrates at or near the dye front. When incubated with core, the band corresponding to the free His-tagged σ^{70} is no longer detected when the gel is stained with Coomassie blue (data not shown). When transferred and probed with BNTA to detect the His-tag, the fast-migrating band corresponding to free His-tagged σ^{70} is detected in the lane that had the free His-tagged σ^{70}. In the His-tagged σ^{70} + core lane, two protein bands which migrate much more slowly than free σ^{70} are observed. These bands react with BNTA and with anti-β' MAb. Most likely, these bands correspond to monomeric and dimeric His-tagged σ^{70} holoenzyme. The latter species is present because of the low salt in the gel (*25*). No band corresponding to free His-tagged σ^{70} was detected with BNTA in the holoenzyme lane (data not shown).

Effect of DNA on Protease Activity. We had some concern that adding DNA to the reaction might inhibit the activity of some of the proteases. The addition of the DNA alters the ionic strength of the solution. In addition, the DNA could bind to basic patches on the protease. Therefore, it seemed possible that the addition of DNA might affect the activity of the proteases and might cause an apparent decrease in protease accessibility due to addition of DNA in open promoter complexes.

When DNA was added following digestion of labeled casein with cucumisin but before TCA precipitation, a loss of 18% of the absorbance at 492 nm was seen, so all absorbances for the samples containing DNA were adjusted by this amount. Once this effect was taken into account, most of the proteases showed similar reactivities whether DNA was added or not as listed in Table 1. The greatest effect was seen with papain, but even this resulted in a loss of only 12% of activity. Because such a small difference is unlikely to be noticed on the film, no adjustments for changes in protease activity were made in the samples containing open complexes.

Footprints of His-tagged σ^{70} Complexes. BNTA detection after Tris−Tricine SDS−PAGE of digestions of C-His-tagged σ^{70} (Figure 1a) and N-His-tagged σ^{70} (Figure 1b) in free, holo, and open promoter complex forms is shown in Figure 1. While nine different proteases were tried, the digestions with cucumisin, papain, and thermolysin for N-His and with bromelain, cucumisin, and elastase for C-His exhibited all bands that could be determined to be unique at the resolution provided in this system, and so only those are shown here. Additional sets of samples were generated using this subset of proteases, and the results for all trials were used to determine the site and level of susceptibility to protease. The exact number of trials for each cleavage is specified under Discussion. All trials showed the same relative levels of susceptibility except for the papain cut near residue 500. Two samples showed the pattern seen in Figure 1b. A third showed no cleavage of free σ^{70}.

Using the size markers generated from chemical digests of His-tagged σ^{70}, it is possible to map the cleavage sites along a linear schematic of the σ^{70} polypeptide as in Figure 2. This summary also includes bands of low signal strength that become detectable upon longer exposure to X-ray film. Also included in Figure 2 are the results obtained using hydroxyl radical cleavage (*26*) and important features of σ^{70},

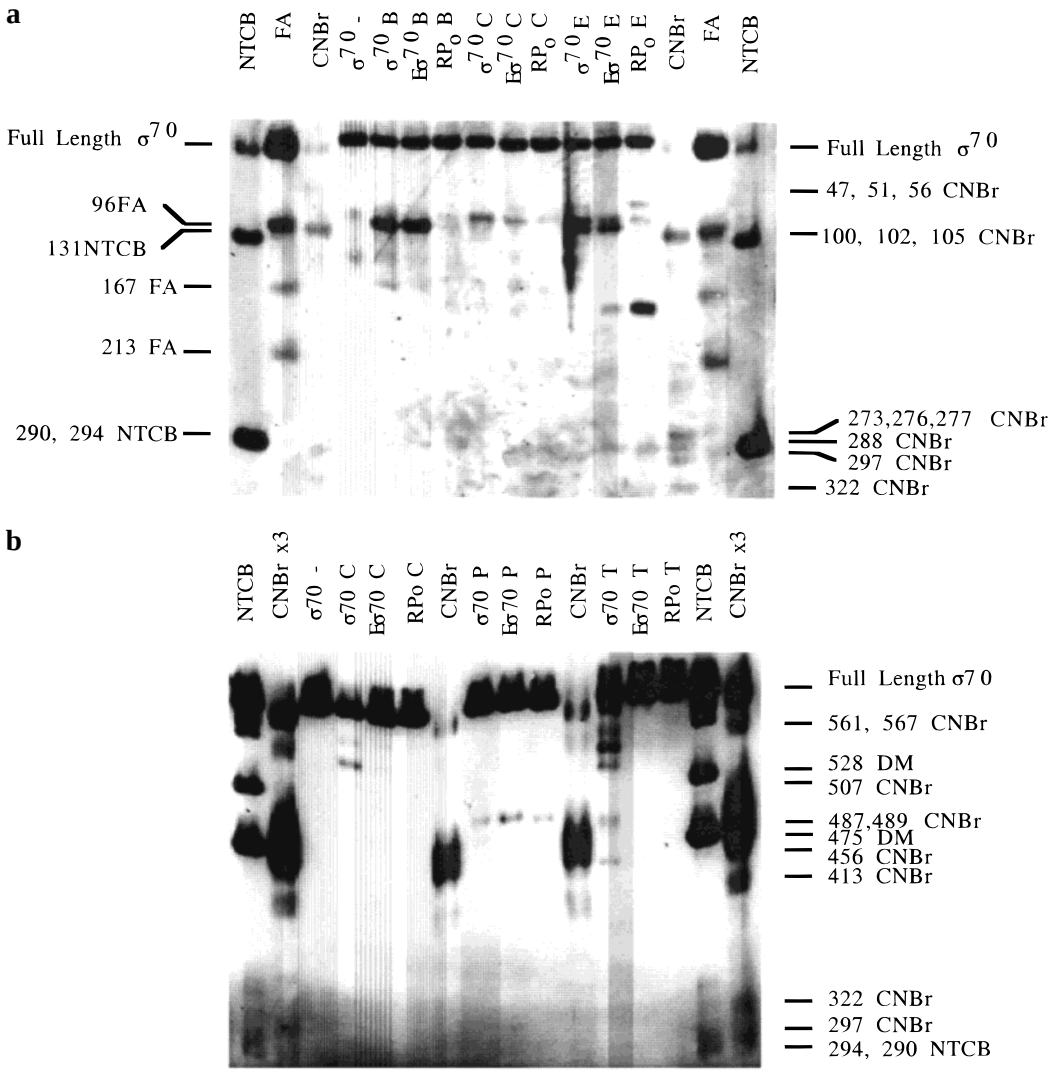

FIGURE 1: Footprinting of His-tagged σ^{70}. Tris−Tricine SDS−PAGE followed by BNTA detection was used to analyze (a) C-terminally or (b) N-terminally His-tagged σ^{70} free in solution (σ^{70}), bound to core RNA polymerase (Eσ^{70}), and in the open promoter complex (RP_o) subjected to limited proteolysis using bromelain (B), cucumisin (C), elastase (E), papain (P), or thermolysin (T) as described under Experimental Procedures. Markers generated by chemical cleavage with NTCB, CNBr, and formic acid (FA) were used as size standards. The sites of these known cleavages are indicated along the sides. As a control, σ^{70} that had not been subjected to proteolysis was run in the lane labeled σ^{70} (−). X-ray film exposure times were (a) 1 min and (b) 15 s.

including the role of region 1 in inhibition of σ^{70}−DNA interactions (*27*) and facilitation of open promoter complex formation (*28*), the role of region 2.1 in core binding (*8*), the role of region 2.3 in single-stranded DNA binding (*29, 30*), the role of region 2.4 in recognition of the promoter −10 region (*31*−*38*), and the role of region 4.2 in recognition of the −35 hexamer of a promoter (*33, 35*). Below these features are shown regions of structural significance, including a region high in acidic amino acid side chains (*24*), a region resistant to trypsin cleavage (*39, 40*), and two putative helix−turn−helix structures (*41*). At the bottom of the figure is shown the location of α-helices determined by X-ray diffraction studies of a crystal of the trypsin-resistant region (*7*) shown as open boxes and those predicted by the PHD computer program shown as stipled boxes (*42*).

This footprinting method produces cleavage sites flanking the protease-resistant fragment seen when using trypsin (*40*). The cleavage defining the N-terminus of this fragment shows a slight increase going from free σ^{70} to holoenzyme and a marked decrease upon open complex formation. The proteolysis site around 448, at the C-terminus of the protease-resistance fragment, drops below the detection limits of this assay upon σ binding to core and is also not seen in the open complex. In addition to these sites, a cleavage site was also seen between regions 1.1 and 1.2 in the open complex, just to the N-terminal side of the protease-resistance fragment. Protease susceptibility at this site decreases as the protein progresses from free σ^{70} or holoenzyme to open promoter complex. Proteolysis is also seen near the highly acidic region between regions 1.2 and 2.1 which increases as the protein progresses through the cycle from almost no cleavage of free σ^{70} to strong cleavage in the open complex. Region 3 has two sites of cleavage: one which decreases upon σ^{70} binding to core polymerase and another which increases upon binding to core polymerase. Another site that shows a decrease in susceptibility upon binding to core is seen C-terminal to region 4.

DISCUSSION

Protein footprinting has gained in popularity since it was first introduced in 1994 (*43*). As with nucleic acid footprinting, the option of either enzymatic digestion or hydroxyl

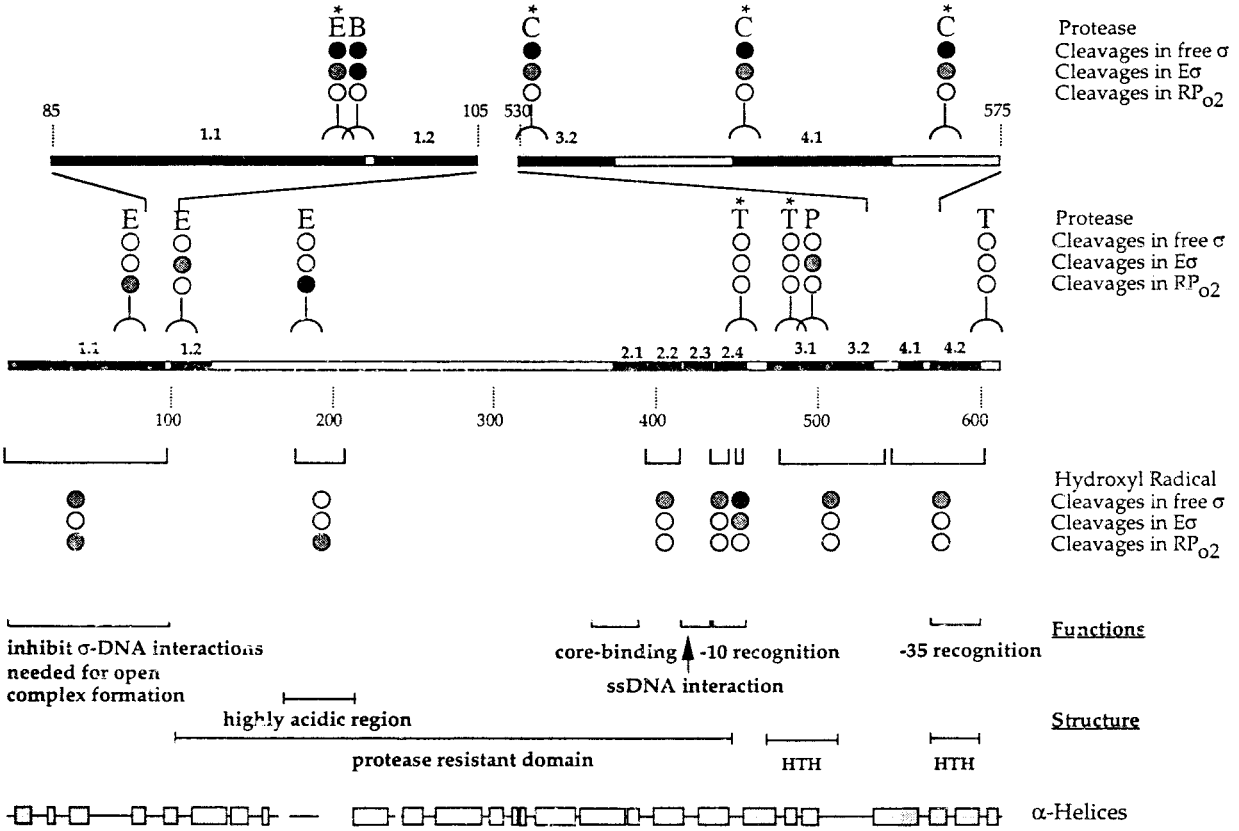

FIGURE 2: Linear map of σ^{70} showing sites of protease susceptibility relative to important functional and structural features. The polypeptide chain of σ^{70} is represented as a box. Above this box, a graphical representation of the results obtained in this study is shown. Sites where cleavage was detected in at least one complex are shown with semicircular arcs. The circles above the arcs show relative levels of cleavage of the different complexes with free σ^{70} on the top, holoenzyme in the middle, and open promoter complex at the bottom. Higher protease susceptibility is indicated by the increasing degree to which the circle is filled. An open circle indicates no detectable cleavage. A black circle indicates strong cleavage observed. Above the indicators for protease susceptibility levels are one-letter abbreviations indicating the protease generating the cleavage. These abbreviations are as given in Figure 1. An asterisk above the protease abbreviations is used to indicate sites generated by multiple proteases. Below the diagram for σ^{70} are shown the results obtained using hydroxyl radical cleavage (*26*) using the same symbols to indicate relative levels of susceptibility. It should be emphasized that the level indicators only represent qualitative levels relative to the same site in other complexes. See the text for an explanation of the functional and structural features of σ^{70} shown below the proteolysis susceptibility indicators.

radical digestion is available to researchers. Hydroxyl radicals react with surface-exposed residues nonspecifically and independent of protein secondary structure. For enzymatic digestion, a cleavage site must have appropriate residues for the protease to recognize and be able to fit into the binding site of the protease in addition to being surface-exposed. Thus, hydroxyl radicals are a better probe for surface-exposed residues while proteases are a better probe for conformational changes within the protein.

Because of an internal σ^{70} kinase site (Cathy Chan, personal communication) and the lack of an appropriate monoclonal antibody for the C-terminus of σ^{70}, we chose a new method of fragment detection, involving the detection of a His-tag appended to either terminus of the protein. Plasmids allowing such constructs are widely available, and the synthesis of BNTA for the detection of histidine tags is quite simple (*20*). Commercial sources of His-tag detection methods are also now available, making this method even easier. In the case of σ^{70}, concern over adverse effects due to the addition of a His-tag is minimal, since both constructs used in this study are able to replace wild-type σ^{70} in vivo (Lin Rao, personal communication).

Because of the concern of hydroxyl radical quenching by the λP_R promoter fragment and the oxidation of the indole rings of the histidine tags, we chose to use an enzymatic approach. To minimize the chance of overlooking protease susceptible sites, nine different proteases with differing specificities (see Table 1) were originally tested.

A final issue for these studies was determining the amount of protein actually in the intended complexes. We began by using molar excesses of core and promoter to help drive all σ^{70} into the intended complex. Native gels were used to determine how much His-tagged σ^{70} was bound to core enzyme. Because σ^{70} is a very acidic protein with a calculated p*I* of 4.5, it has a very high mobility rate on native gels. When bound to the much larger and less acidic core polymerase, σ^{70} migrates much slower. Thus, comparing free σ^{70} to σ^{70} as part of holoenzyme would be similar to a gel shift assay. We found this to be the case, and observed that under the conditions used, no detectable free σ^{70} was present (data not shown).

Another concern was the binding of holo RNA polymerase to promoter. RNA polymerase is known to have affinity for ends of linear DNA as well as nonspecific internal sites (see *44* and references contained therein). To make sure that most of the His-tagged σ^{70} was in the open complex upon adding promoter fragment, we used a strong, well-characterized promoter and conditions known to favor open complex

formation. From the cleavage results with bromelain and elastase (Figure 1a), it is clear that some DNA-induced conformational change occurs. This effect was seen in every independently generated proteolysis ladder (at least eight for each protease). The consistency with which this effect was generated suggests that the same complex is present in the other samples, even if no conformational change is evident.

Mapping of Protease Susceptible Sites of His-tagged σ^{70} Complexes. Reading along the length of the polypeptide chain starting with the N-terminus, the first site we found maps to residue 78 ± 13 ($n = 4$ independent gels) which places it in region 1.1. This site is not cleaved in the free σ^{70} or holoenzyme, but only in the open complex. While σ^{70} has DNA binding regions, free σ^{70} does not bind to DNA. However, deletion mutants lacking this region are able to bind DNA (*27*). This suggests that region 1.1 occupies a site that blocks some of the DNA binding domains. The DNA binding sites are accessible while σ^{70} is in the holoenzyme form, suggesting that σ^{70} undergoes a conformational change that results in region 1.1 no longer occupying the site that blocks the DNA binding domains. Region 1.1 also plays a role in open complex formation (*28*). In the open complex, this region becomes slightly accessible to elastase, indicating that it undergoes a second conformational change.

Close to the start of region 1.2, a number of cleavage sites are detected (96 ± 10, $n = 4$; 98 ± 9, $n = 3$; and 107 ± 9, $n = 4$) and have been previously seen for free σ^{70} (*40, 45*). These sites are less sensitive in the open complex. Based on the model that σ^{70} is a flexible protein with hinge regions, and that cleavage at this site allows crystallization (*40*), it seems possible that this region might be a hinge that becomes less susceptible to protease attack as σ^{70} isomerizes during the course of its cycle. It has been shown (*28*) that region 1 is necessary for the isomerization that precedes initiation of transcription. The change in susceptibility at this hinge may be a result of this isomerization. In the open complex, the hinge adopts a conformation that is less susceptible to proteolysis.

The next region of protease susceptibility occurs close to the highly acidic region of σ^{70} at residue 191 ± 7 ($n = 4$). This site lies in the region of σ^{70} that has been crystallized. The acidic region itself is disordered in the crystal but appears to be close to the DNA binding site at region 2.4 (*7*). Based on this, it was proposed (*7*) that this region might sterically and electrostatically inhibit DNA binding and that this region must be displaced before promoter DNA can bind. This region shows little protease susceptibility in free σ^{70}, shows increased susceptibility in holoenzyme, and becomes very susceptible in the open promoter complex. We propose that this region undergoes two conformational changes. In free σ^{70}, the acidic region is closely associated with the DNA binding site which sterically hinders the proteases, preventing cleavage in this conformation. Upon binding to core, this acidic region is further away from the DNA binding site, relieving some steric hindrance and opening up region 2.4 to bind to the −10 region of the promoter. Once the promoter is bound, the acidic region of σ^{70} moves even further out, allowing elastase much better access to this site. This may be due to electrostatic repulsion between the DNA and the acidic region. It would be interesting to see how the cleavage pattern of σ^{70} from *E. coli* C differs from that of *E. coli* K12 used here, since *E. coli* C lacks a stretch of 10 consecutive acidic residues in the highly acidic region (*46*).

The next protease susceptible site we see is near 448 (446 ± 6, $n = 2$), the cleavage site seen previously with trypsin (*40*). This site is undetectable in holoenzyme or the open complex. When trypsin is used in this method, it produces a fragment which is indistinguishable from the thermolysin cut shown here and also decreases when σ^{70} is bound to core and in the open complex (data not shown). Therefore, we think that the thermolysin cleavage site is also near residue 448. In the crystal structure, this region maps very close to region 2.1 (*7*), a region shown to be important for core binding of σ^{70} (*8*). Considering the fact that core RNA polymerase is a 380 kDa protein, it is not surprising that this site is blocked upon binding to core.

The next two sites map within region 3, near position 500 (486 ± 7, $n = 5$; and 486 ± 8, $n = 3$). Though these two sites map close together, they show different susceptibility depending on the step in the σ^{70} cycle. The site generated by thermolysin is only detected for free σ^{70}. The site generated by papain shows an increase going from free σ^{70} to the holoenzyme. The homologous region in *Bacillus subtilis* σ^{D} is also susceptible to limited proteolysis (*47*) and is cleaved in free σ^{70} (*7*) although the 500−613 fragment was quickly digested to smaller fragments. This 500−613 fragment was stabilized in the presence of the T4 bacteriophage protein AsiA (*40*). The fact that two sites mapping so closely together would have such different susceptibilities seems to indicate that this region undergoes large conformational changes.

Finally, there is a stretch of four cleavage sites mapping past the 500 site and continuing to near the C-terminus (531 ± 7, $n = 7$; 552 ± 9, $n = 7$; 572 ± 10, $n = 7$; 600 ± 2, $n = 3$). All four of these sites are apparent in free σ^{70}, but show little to no cleavage in the holoenzyme and none in the open complex in Figure 1b. Longer film exposure times show the level of cleavage at these sites decreases when σ^{70} is part of the holoenzyme and further decreases when bound in the open complex. This region of σ^{70} includes the part of the protein that recognizes the −35 region of the promoter (*33, 35*). It has been shown that the C-terminal third of the α-subunit can bind to promoter DNA around −42 relative to the start of transcription (*48*), just upstream of the −35 region. We have previously shown that σ^{70} can be cross-linked to the C-terminal one-third of α (*21*) which includes the DNA binding site (*49, 50*). We therefore think that at least part of the protection seen here due to core enzyme is provided by this region of α. This could be tested by performing similar experiments with core RNA polymerases lacking the C-terminal domain of α.

In Figure 3, we present a very schematic model of σ^{70} conformational changes that is consistent with the changes in protease susceptibility reported here. In this model, free σ^{70} is shown as having two hinges separating three structural domains. Region 1.1 is positioned such that it can interfere with DNA binding to either region 2.4 or region 4.2.

Upon binding to core enzyme, both hinges undergo a conformational change to account for changes in their protease susceptibilities. Region 1.1 changes its position to open up the DNA binding domains. The regions C-terminal to residue 448 are shown as being partially protected by core to digestion by cucumisin and thermolysin. Finally, the acidic

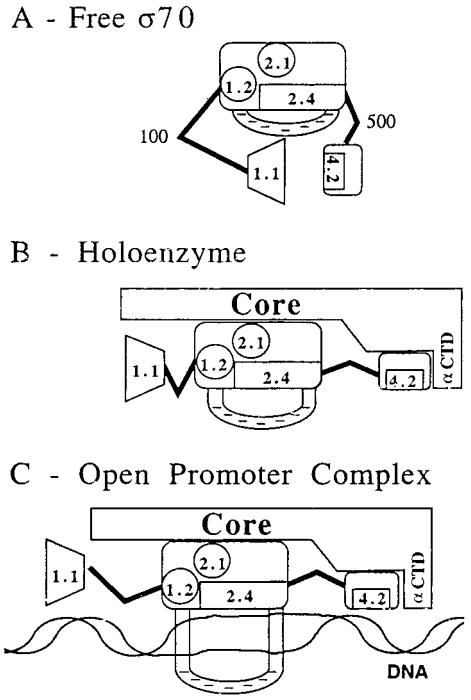

FIGURE 3: Model of σ^{70} conformational changes. (A) Free σ^{70}. The protease resistant domain of σ^{70} is shown as a central box with the remainder of the protein connected by a pair of flexible hinges. The central axes of the α-helices of regions 1.2 and 2.1 are perpendicular to the plane of the figure, while the axis of the region 2.4 α-helix runs horizontally. The highly acidic region between region 1 and region 2 is shown as a loop of negative charges. Also indicated are region 1.1 and the putative −35 recognition α-helix of the putative helix−turn−helix motif of region 4.2. (B) Holoenzyme. Core is shown as a large polygon binding to σ^{70} at region 2.1 and other places. For simplicity, only the regions of core interacting with σ^{70} are shown. A region of the core enzyme corresponding to one of the two αCTDs is also indicated. (C) Open complex. Promoter DNA is shown as a helix binding to regions 2.4 and 4.2 of σ^{70} with a melted out region near region 2.4 of σ^{70}. See the text for a more detailed explanation of the conformational changes shown.

loop is shown as extending out further from the protease-resistant domain, explaining its increased cleavage by elastase.

When σ^{70} is in the open promoter complex, additional changes occur. Region 1.1, which is necessary for open complex formation and is cleaved by elastase in the open complex, is shown as extending away from the core enzyme and DNA to explain the cleavage seen near residue 78 in the open promoter complex. The DNA is shown as partially protecting the two hinges, representing the loss of proteolysis seen in these areas upon DNA binding. The acidic region is shown as extending out even further from the protease resistant core. This change is perhaps the most striking we observed because it involves a site that is relatively inaccessible to protease in free σ^{70} and holoenzyme but which becomes quite accessible in the open complex. This strongly implies a significant conformational change. In many of the other sites, accessibility becomes less in the open complex, and it is not easy to determine if this is due to a conformational change in a site or merely steric exclusion of the protease by the bound DNA.

Although we used a large number of proteases with differing specificities, we were unable to see any cleavage of free σ^{70} between residues 114 and 448. The existence of a fragment of σ^{70} that was highly resistant to a number of proteases was first reported many years ago (*45*). This resistant fragment, when generated by trypsin, spans residues 114−448 (*40*). This study includes five proteases that were not used in the study by Gribskov, none of which cleaved this region of free σ^{70} in this assay. It seems clear that in the native form, this fragment of σ^{70} is protected from endoproteases. X-ray diffraction studies of a crystal of this protease-resistant domain show the region to consist mostly of α-helices and to include two 2-stranded coiled-coils. Presumably, it is these structural features that protect this fragment from proteolytic attack.

Recently a report was published which used hydroxyl radicals to footprint σ^{70} (*26*). This report tested the same complexes as we did, and the results are summarized in Figure 2. There is good agreement between the two methods. Each shows a pattern of general protection of Eσ^{70} for the four regions of homology shared among primary σ factors. Both methods indicate that region 1.1 and the acidic region become more susceptible to cleavage in the open promoter complex relative to Eσ^{70}. The major differences between the two studies are that the hydroxyl radical method provided information along the entire length of the polypeptide chain, while the protease method only examined isolated sites, and that the protease studies allow for greater speculation about conformational changes.

Though the data from free σ^{70} and the open promoter complex are in close agreement, there are some discrepancies between the two procedures with respect to the holoenzyme. The protease method shows three general sites where susceptibility increases upon binding to core polymerase. These positions are near the boundary between subregions 1.1 and 1.2, near the acidic region, and in the middle of region 3.1. The hydroxyl radical method showed two regions of increased cleavage in the holoenzyme relative to free σ^{70}. One was near the acidic region, in agreement with our elastase results. The other was in region 4.2 in one of the putative α-helices of the helix−turn−helix motif believed to be involved in recognition of the −35 region of the promoter. This discrepancy may be a result of specific target sites having different levels of reactivity toward enzymatic or hydroxyl radical proteolysis.

Similar experiments using proteases for footprinting have been performed on the alternative *E. coli* transcription factor σ^{54} (*51*). Unfortunately, due to a lack of any clear homology between the two proteins, we are unable to make any meaningful comparison between the two sets of data.

Despite the relatively few cuts seen along the length of the σ^{70} polypeptide, the data presented here are quite exciting. We were able to obtain results which support the model that σ^{70} has flexible hinges on either end of the protease resistant domain, as well as the model that the acidic region moves relative to the DNA binding domain of region 2.4 (*7*). We confirmed that regions C-terminal to residue 448 are protected when σ^{70} is bound to core RNA polymerase (*26*), indicating sites of possible secondary interaction between σ^{70} and the core enzyme. We demonstrated that region 1.1 undergoes a conformational change upon entering the open complex, consistent with results that it is required for making this transition (*28*). Finally, we demonstrated the general viability of limited proteolysis of His-tagged proteins followed by BNTA detection of the resulting ladder.

ACKNOWLEDGMENT

We thank the Thomas Record lab for the gift of the strain carrying the pBR81 plasmid, Maria Fremlin for purifying some of the core used in these experiments, and Kit Nolan for the monoclonal antibodies used. We also thank Rachel Mooney for advice on large-scale PCR.

REFERENCES

1. Gross, C. A., Lonetto, M., and Losick, R. (1992) in *Transcription Regulation* (McKnight, S., and Yamamoto, K., Eds.) pp 129−176, Cold Spring Harbor Press, Cold Spring Harbor, NY.
2. Travers, A. A., and Burgess, R. R. (1969) *Nature 222*, 537−540.
3. Burgess, R. R., Travers, A. A., Dunn, J. J., and Bautz, E. K. (1969) *Nature 221*, 43−46.
4. Heil, A., and Zillig, W. (1970) *FEBS Lett. 11*, 165−168.
5. Record, M. T., Jr., Reznikoff, W. S., Craig, M. L., McQuade, K. L., and Schlax, P. J. (1996) in *Escherichia coli and Salmonella* (Neidhardt, F. C., Ed.) pp 792−821, ASM Press, Washington, D.C.
6. Suh, W. C., Leirmo, S., and Record, M. T., Jr. (1992) *Biochemistry 31*, 7815−7825.
7. Malhotra, A., Severinova, E., and Darst, S. A. (1996) *Cell 87*, 127−136.
8. Lesley, S. A., and Burgess, R. R. (1989) *Biochemistry 28*, 7728−7734.
9. Zhou, Y. N., Walter, W. A., and Gross, C. A. (1992) *J. Bacteriol. 174*, 5005−5012.
10. Joo, D. M., Ng, N., and Calendar, R. (1997) *Proc. Natl. Acad. Sci. U.S.A. 94*, 4907−4912.
11. Joo, D. M., Nolte, A., Calendar, R., Zhou, Y. N., and Jin, D. J. (1998) *J. Bacteriol. 180*, 1095−1102.
12. Kaneda, M., Yonezawa, H., and Uchikoba, T. (1995) *Biotechnol. Appl. Biochem. 22*, 215−222.
13. Keil, B. (1992) *Specificity of Proteolysis*, Springer-Verlag, Berlin.
14. Rao, L., Jones, D. P., Nguyen, L. H., McMahan, S. A., and Burgess, R. R. (1996) *Anal. Biochem. 241*, 173−179.
15. Nguyen, L. H., Jensen, D. B., and Burgess, R. R. (1993) *Protein Expression Purif. 4*, 425−433.
16. Gribskov, M. R., and Burgess, R. R. (1983) *Gene 26*, 109−118.
17. Suh, W. C., Ross, W., and Record, M. T., Jr. (1993) *Science 259*, 358−361.
18. Thompson, N. E., Hager, D. A., and Burgess, R. R. (1992) *Biochemistry 31*, 7003−7008.
19. Burgess, R. R., and Jendrisak, J. J. (1975) *Biochemistry 14*, 4634−4638.
20. McMahan, S. A., and Burgess, R. R. (1996) *Anal. Biochem. 236*, 101−106.
21. McMahan, S. A., and Burgess, R. R. (1994) *Biochemistry 33*, 12092−12099.
22. Khalkhali-Ellis, Z. (1995) *Prep. Biochem. 25*, 1−9.
23. Strickland, M. S., Thompson, N. E., and Burgess, R. R. (1988) *Biochemistry 27*, 5755−5762.
24. Burton, Z., Burgess, R. R., Lin, J., Moore, D., Holder, S., and Gross, C. A. (1981) *Nucleic Acids Res. 9*, 2889−2903.
25. Shaner, S. L., Piatt, D. M., Wensley, C. G., Yu, H., Burgess, R. R., and Record, M. T., Jr. (1982) *Biochemistry 21*, 5539−5551.
26. Nagai, H., and Shimamoto, N. (1997) *Genes Cells 2*, 725−734.
27. Dombroski, A. J., Walter, W. A., Record, M. T., Jr., Siegele, D. A., and Gross, C. A. (1992) *Cell 70*, 501−512.
28. Wilson, C., and Dombroski, A. J. (1997) *J. Mol. Biol. 267*, 60−74.
29. Huang, X., Lopez de Saro, F. J., and Helmann, J. D. (1997) *Nucleic Acids Res. 25*, 2603−2609.
30. Juang, Y.-L., and Helmann, J. D. (1994) *J. Mol. Biol. 235*, 1470−1488.
31. Daniels, D., Zuber, P., and Losick, R. (1990) *Proc. Natl. Acad. Sci. U.S.A. 87*, 8075−8079.
32. Jones, C. H., Tatti, K. M., and Moran, C. P., Jr. (1992) *J. Bacteriol. 174*, 6815−6821.
33. Kenney, T. J., and Moran, C. P., Jr. (1991) *J. Bacteriol. 173*, 3282−3290.
34. Kenney, T. J., York, K., Youngman, P., and Moran, C. P., Jr. (1989) *Proc. Natl. Acad. Sci. U.S.A. 86*, 9109−9113.
35. Siegele, D. A., Hu, J. C., Walter, W. A., and Gross, C. A. (1989) *J. Mol. Biol. 206*, 591−603.
36. Tatti, K. M., Jones, C. H., and Moran, C. P., Jr. (1991) *J. Bacteriol. 173*, 7828−7833.
37. Waldburger, C., Gardella, T., Wong, R., and Susskind, M. M. (1990) *J. Mol. Biol. 215*, 267−276.
38. Zuber, P., Healy, J., Carter, H. L., Cutting, S., Moran, C. P., and Losick, R. (1989) *J. Mol. Biol. 206*, 605−614.
39. Lowe, P. A., Hager, D. A., and Burgess, R. R. (1979) *Biochemistry 18*, 1344−1352.
40. Severinova, E., Severinov, K., Fenyo, D., Marr, M., Brody, E. N., Roberts, J. W., Chait, B. T., and Darst, S. A. (1996) *J. Mol. Biol. 263*, 637−647.
41. Gribskov, M. R., and Burgess, R. R. (1986) *Nucleic Acids Res. 14*, 6745−6763.
42. Rost, B., and Sander, C. (1993) *J. Mol. Biol. 232*, 584−599.
43. Heyduk, E., and Heyduk, T. (1994) *Biochemistry 33*, 9643−9650.
44. Roe, J. H., Burgess, R. R., and Record, M. T., Jr. (1984) *J. Mol. Biol. 176*, 495−522.
45. Gribskov, M. R. (1985) Ph.D., University of Wisconsin−Madison.
46. Christie, G. E., and Cale, S. B. (1995) *Gene 162*, 161−162.
47. Chen, Y. F., and Helmann, J. D. (1995) *J. Mol. Biol. 249*, 743−753.
48. Ross, W., Gosink, K. K., Salomon, J., Igarashi, K., Zou, C., Ishihama, A., Severinov, K., and Gourse, R. L. (1993) *Science 262*, 1407−1413.
49. Gaal, T., Ross, W., Blatter, E. E., Tang, H., Jia, X., Krishnan, V. V., Assa-Munt, N., Ebright, R. H., and Gourse, R. L. (1996) *Genes Dev. 10*, 16−26.
50. Jeon, Y. H., Negishi, T., Shirakawa, M., Yamazaki, T., Fujita, N., Ishihama, A., and Kyogoku, Y. (1995) *Science 270*, 1495−1497.
51. Casaz, P., and Buck, M. (1997) *Proc. Natl. Acad. Sci. U.S.A. 94*, 12145−12150.

BI990824X